Accelerated Publications

Selective Isotopic Enrichment of Synthetic RNA: Application to the HIV-1 TAR Element†

Malgorzata J. Michnicka,‡ J. Wade Harper,§ and Garry C. King*,‡

W. M. Keck Center for Computational Biology, Department of Biochemistry and Cell Biology, Rice University, 6100 South Main Street, Houston, Texas 77005, and Verna and Marrs McLean Department of Biochemistry, Baylor College of Medicine, One Baylor Plaza, Houston, Texas 77030

Received November 4, 1992; Revised Manuscript Received December 2, 1992

ABSTRACT: The introduction of isotopically enriched nucleotides into NMR quantities of a synthetic 29-mer RNA derived from the HIV-1 TAR element is described. RNA enriched in ^{13}C and/or ^{15}N is produced by a procedure which involves isolation of whole cellular RNA from *Escherichia coli*, nucleolysis, separation of mononucleotides, chemical or enzymatic pyrophosphorylation, and in vitro transcription by T7 RNA polymerase. Spectral characteristics of each residue type are examined in isolation. ^{13}C chemical shifts provide an alternative method to determine ribose puckers for larger RNAs. Nonprotonated sites such as purine N7 groups can now be monitored through the use of multiple-bond ^{1}H–^{15}N coupling. When applied conservatively, coordinate analysis of chemical shift values should prove valuable for NMR studies of RNA structure and recognition. ^{1}H, ^{13}C, and ^{15}N chemical shift data suggest that TAR residue A35 has an unusual local environment, consistent with extrusion of its base from the terminal loop.

The recent surge in the application of heteronuclear NMR techniques to protein structural studies has been fueled by two factors: the development of multidimensional indirect-detection methods and the availability of protein expression systems to facilitate the introduction of ^{15}N and ^{13}C labels. Since heteronuclear methods offer powerful approaches to the structure, dynamics, and interactions of macromolecules, a straightforward method for labeling nucleic acids should also find considerable application. This is particularly true for NMR analysis of RNAs such as ribozymes, ribosomal RNAs, transfer RNAs, and genetic control elements, which fold into relatively compact structures containing bulges, loops, pseudoknots, and duplex regions (Wyatt et al., 1989). ^{1}H NMR spectra of RNAs typically display severe overlap of their ribose signals [see Varani and Tinoco (1991a)], making ^{13}C enrichment almost essential for detailed application of NMR to molecules in the 30–100-mer (10–30 kDa) range. In addition, ^{15}N labeling offers the prospect of improved experimental access to Watson–Crick and other hydrogen-bonding phenomena.

Labels may be introduced in a uniform or selective fashion, depending upon the experimental system and the information desired. Uniform enrichment with ^{15}N has been previously applied to natural RNAs in vivo, including 5S rRNA fragments (Kime, 1984; Gewirth et al., 1987), while selective ^{15}N labeling has been used to monitor the N1 and N3 signals of bases from tRNA and 5S rRNA (Roy et al., 1984; Griffey et al., 1985; Davis et al., 1989). Various atomic sites in bacterial tRNAs have also been monitored following selective ^{13}C introduction (Yokoyama et al., 1980; Olsen et al., 1982; Schmidt et al., 1987). In these earlier studies, selective enrichment was typically achieved by growth of auxotrophs in the presence of labeled compounds prepared by chemical synthesis. The development of methods for in vitro RNA labeling, which is applicable to a much wider variety of RNA species, has recently been pursued in several laboratories (Nikonowicz & Pardi, 1992; Santoro & King, 1992; Nikonowicz et al., 1992; Batey et al., 1992). While other groups have demonstrated the utility of uniform enrichment, our own efforts have initially centered on labeling by residue type, where extensive spectral simplification can be achieved while retaining the ability to perform connectivity analysis.

This paper describes a procedure which can be used to produce milligram quantities of synthetic RNA labeled selectively by residue type. As an illustration of the approach, we present NMR spectra of a 29-mer derived from the trans activator regulatory (TAR) element of HIV-1, a bulged hairpin structure (Figure 1) which plays a critical role in the regulation of viral transcription (Rosen et al., 1985). Initial predictions of a three-base bulge/six-base loop structure for TAR (Muesing et al., 1987) have been followed by a number of newly proposed models for the conformations of these two regions (Colvin & Garcia-Blanco, 1992; Delling et al., 1992; Puglisi et al., 1992; Loret et al., 1992), some of which are apparently contradictory. With the example provided by the TAR 29-mer, we discuss methods by which previously unused or unobserved heteronuclear NMR data can assist in RNA structure determination, clarify structural ambiguities, and make additional contributions to analysis of ligand binding.

MATERIALS AND METHODS

Whole Cellular RNA. Six 1-L cultures of *Escherichia coli* K561 or MRE600 (ATCC 29417) were grown in M9 medium at 37 °C with vigorous shaking. The sole carbon and/or nitrogen sources for labeling with one or both isotopes were

† Supported by grants from the National Institutes of Health (GM-42913 to G.C.K. and AI-29833 to J.W.H.) and the Welch Foundation (C-1166 to G.C.K.) and an American Cancer Society Junior Faculty Award to J.W.H. Establishment of the Rice 500-MHz NMR facility was supported by NIH Grant RR-05759 and the W. M. Keck Foundation.

* Corresponding author.
‡ Rice University.
§ Baylor College of Medicine.

0006-2960/93/0432-395$04.00/0 © 1993 American Chemical Society

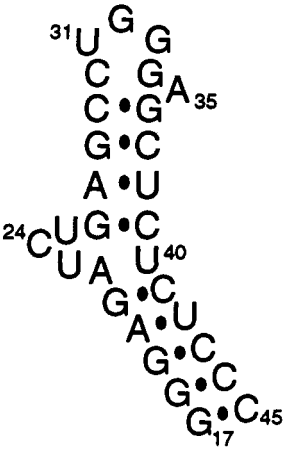

FIGURE 1: Nucleotide sequence of ΔTAR29.1, drawn to emphasize structural features identified by NMR. Watson–Crick base pairs for which imino proton resonances can be observed at 30 °C are indicated by filled circles.

0.5 g/L [$^{13}C_6$]glucose (95–99%) and/or 0.5 g/L [^{15}N]-ammonium chloride (99%) respectively. Cultures were grown to late log phase and harvested by centrifugation at 6000*g* for 10 min. Cell pellets were suspended at 2 g of wet-packed cells per liter in 15 mM Tris·HCl, 0.45 M sucrose, and 8 mM EDTA, pH 8.0, and 20 mg of lysozyme was added before standing on ice for 20 min. Protoplasts were collected by centrifugation at 1300*g* for 5 min, suspended in 300 mL of 10 mM Tris·HCl, 10 mM NaCl, 1 mM sodium citrate, 1.5% SDS,[1] 0.05% DEPC, pH 8.0, heated to 37 °C for 15 min, and cooled on ice. DNA, protein, and SDS were precipitated by gentle addition of one-half volume of saturated NaCl, incubation on ice for 10 min, and centrifugation at 30000*g* for 15 min. Supernatant RNA was precipitated with 2.5–3 volumes of ethanol, stood overnight at –20 °C, and collected by centrifugation at 22000*g* for 15 min.

Nucleoside 5'-Monophosphates. Cellular RNA was suspended at 0.5–1.0 mg/mL in 30 mM sodium acetate, 0.1 mM $ZnCl_2$, pH 5.0, heated to 90 °C for 5 min, quick-cooled, and incubated at 37 °C overnight with 30 units of S_1 or 3 units of P_1 nuclease/mg of RNA before finally heating to 90 °C for 5 min. Digestion was monitored by denaturing (7 M urea) PAGE. NMPs were precipitated with 5 volumes of cold acetone, resuspended at 50–100 mM in water, and reprecipitated with two volumes of ethanol.

For separation of NMPs, the ethanol precipitate was resuspended in water and subjected to ion-exchange HPLC on a 10 min × 125 mm Nucleogen DEAE 60-7 column (Macherey Nagel) with a pellicular guard (405/WAX, Custom LC, Inc.) or chromatography on a 15 × 2.5 cm column of DEAE-trisacryl (EM Science). A linear gradient of 0.04–0.80 M triethylamine–acetic acid, pH 4.0, was applied for elution. Pooled NMP fractions were concentrated by rotary evaporation and ethanol precipitated. Purity was checked by NMR.

Nucleoside 5'-Triphosphates. Triphosphorylation was performed by chemical or enzymatic means. For the chemical method, 1 equiv of tributylamine was added to the NMP sample before drying by repeated evaporation of anhydrous DMF. Tributylammonium NMPs were dissolved to 0.1 M in DMF, and a 5-fold excess of 0.5 M 1,1'-carbonyldiimidazole in DMF was added before the sealed reaction tubes were allowed to stand in a dessicator overnight. Eight equivalents of methanol were added, followed 2–3 h later by 5 equiv of 0.2 M tributylammonium pyrophosphate in DMF, and the mixture stood overnight. Any precipitate present after incubation was dissolved by addition of cold, sterile water. Pure NTPs were obtained by HPLC on a Nucleogen 60-7 column, eluted with a linear gradient of 40 mM–1.2 M ammonium acetate, pH 7, over 45 min. Pooled NTP fractions were dried, resuspended, and precipitated with ethanol.

For the enzymatic method, mononucleotides were dissolved to a concentration near 200 mM in 50 mM Tris·HCl and 10 mM DTT, pH 7.4. Three equivalents of PEP and 1 equiv of $MgCl_2$ were added in concert with enzymes. Individual phosphorylation of AMP, CMP, GMP, and UMP was achieved with 250 units/mL adenylate kinase, 900 units/mL adenylate kinase, 3 units/mL guanylate kinase, and 1300 units/mL adenylate kinase, respectively, plus 50–250 units/mL pyruvate kinase and 0.5 mM unlabeled ATP in all cases. Mixed NMPs were phosphorylated in a mixture containing 250 units/mL adenylate kinase, 3 units/mL guanylate kinase, 5 units/mL pyruvate kinase, and 0.5 mM ATP. Reaction progress was monitored by polyethyleneimine cellulose TLC, with occasional pH adjustment (0.1 M HCl) and further addition of enzymes if indicated. NTPs were precipitated with ethanol and used without further purification.

RNA Synthesis. NMR-scale in vitro RNA production was performed in 5–10 mL of 40 mM Tris·HCl, 10 mM DTT, 8 mM $MgCl_2$, 50 mM NaCl, and 1 mM spermidine, pH 8.0, with plasmid template and T7 RNA polymerase concentrations of 200 and 400 nM, respectively. For selective labeling, NTP concentrations were 1 mM for the single enriched species and 2 mM for the others. Template DNA was obtained by *Sma*I linearization of pΔTAR, a pUC19-derived vector carrying a 17 bp T7 RNA polymerase promoter fused to the coding sequence for ΔTAR29.1, a 29-mer derived from residues 17–45 of the HIV-1 LAI TAR sequence (see Figure 1). Following runoff transcription for 3–8 h at 37 °C, unincorporated nucleotides, abortive transcripts, polymerase, and template were removed by stepwise elution of a 2-mL TSK-DEAE column with 30 mM sodium acetate, pH 6.0, buffer containing 100 and 300 mM NaCl successively. The presence of correct transcript was assessed by denaturing PAGE before ethanol precipitation and resuspension in DEPC-treated water. In some cases, RNA was further purified by HPLC on a 10 × 125 mm Nucleogen 60-7 column, eluted over 30 min with 20 mM sodium acetate and 5 M urea, pH 6.0, and a 300–800 mM KCl gradient. Final yields of labeled ΔTAR29.1 were 3–10 mg.

NMR Sample Preparation and Spectroscopy. Purified RNA samples were dialyzed overnight in DEPC-treated tubing against 4 L of water with a small quantity of added Chelex-100 (Bio-Rad). Dialyzed RNA was vacuum-concentrated to dryness before dissolution in 500 μL of NMR buffer, with three cycles of dissolution in D_2O and vacuum concentration. The standard buffer was 10 mM phosphate, 100 mM NaCl, and 0.1 mM EDTAd_4 (CIL), pH 7.0.

NMR spectra were acquired on a Bruker AMX-500 spectrometer at 30 °C using a 5-mm inverse broad-band probe. Direct ^{13}C and ^{15}N spectra were collected via the decoupling coil. HMQC and HSQC spectra were obtained with standard pulse sequences (Bax et al., 1990) and GARP-1 heteronuclear decoupling.

[1] Abbreviations: DEAE, diethylaminoethyl; DEPC, diethylpyrocarbonate; DMF, dimethylformamide; HMQC, heteronuclear multiple-quantum correlation spectroscopy; HSQC, heteronuclear single-quantum correlation spectroscopy; PAGE, polyacrylamide gel electrophoresis; PEP, phosphoenolpyruvate; SDS, sodium dodecyl sulfate.

RESULTS AND DISCUSSION

Production of Labeled RNAs. The procedures employed here for labeled RNA preparation are based on methods for the isolation of bacterial RNA (Summers, 1970; Gilman, 1987), pyrophosphorylation of NMPs (Hoard & Ott, 1965; Simon et al., 1990), and in vitro RNA synthesis by T7 RNA polymerase (Milligan et al., 1987; Milligan & Uhlenbeck, 1989). Other protocols involving labeled RNA preparation for LC/MS (Polson et al., 1991) and NMR (Nikonowicz et al., 1992; Batey et al., 1992) have appeared recently. Each protocol has its relative merits, detailed discussion of which is beyond the scope of this paper, but it is likely that a refined hybrid method will emerge for general use. Some significant aspects of the present procedure are considered below.

Typical yields of 50–80 mg of RNA/g of glucose are 50–80% of the theoretical maximum based on a yield coefficient of 0.5 for glucose and an RNA content of 20% dry cell mass (Ingraham et al., 1983). The choice of a nuclease for RNA hydrolysis is not critical, but P_1 nuclease has higher general activity. Although an important component of this study, individual NMP separation is not required for many applications (Nikonowicz & Pardi, 1992; Batey et al., 1992). The enzymatic method of NMP pyrophosphorylation (Simon et al., 1990; Nikonowicz & Pardi, 1992) is usually superior to the chemical approach, routinely yielding NTPs of >95% purity. The chemical method (Hoard & Ott, 1965) typically provides yields of 70–80%, but NTPs must be chromatographically separated from reagents and byproducts. Chemical phosphorylation should also find application in the production of enriched dNTPs for enzymatic labeling of DNA and for NMR analysis of enzyme–dNTP interactions. The final distribution of labeled NTPs reflects the relative prevalence of bases in *E. coli* RNA, where the G:A:U:C ratios are approximately 1.6:1.3:1.1:1 (Ingraham et al., 1983). This is helpful in that abortive transcripts which may account for over one-half of the RNA produced tend to be purine-rich.

In this study, selective labeling of ΔTAR29.1 in milligram quantities has been accomplished by runoff transcription from a linearized plasmid template. Plasmid-based transcription involves extra labor over the use of an oligonucleotide template, but in our hands yields a superior product for NMR, frequently needing no purification beyond step-eluted chromatography. We have employed HPLC (Szewczak et al., 1987; Harper & Logsdon, 1991) in cases where further purification is required, but large-scale electrophoresis may also be used. In our hands, in vitro synthesis yields of up to 50% can be obtained for this system. On occasions when total labeling is employed, unincorporated NTPs and abortive transcripts may be recycled readily.

^{13}C NMR of Selectively Labeled ΔTAR29.1. The results reported here are part of an ongoing effort to probe the solution structure and interactions of ΔTAR29.1 RNA using NMR methods. Following a coarse structure determination based upon a subset of assigned ^1H signals (Chang and King, unpublished results), work toward total assignment of all spin $^1/_2$ signals was begun with a view to improving the structure determination through the use of heteronuclear data. The potential utility of selective labeling became apparent in this context, and the three different kinds of secondary structural elements found in ΔTAR29.1 make it an excellent demonstration case. Figure 2 shows the aromatic regions from ^{13}C NMR spectra of ΔTAR29.1 samples labeled by residue type. In general, signal dispersion is reasonably good, ranging between 1.9 and 4.9 ppm for protonated sites and up to 2.7 ppm for nonprotonated sites. Resolved signals from the four

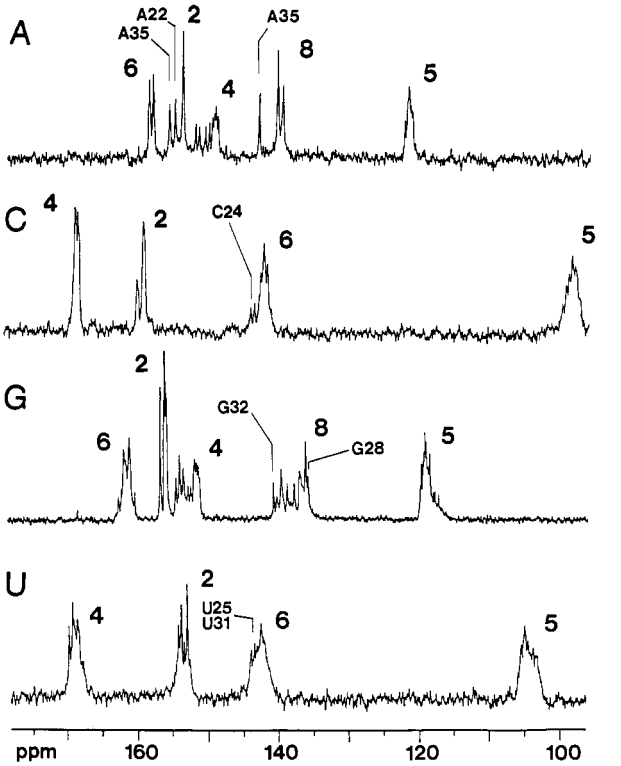

FIGURE 2: Aromatic regions from ^1H-decoupled ^{13}C NMR spectra of ΔTAR29.1 selectively labeled with (top to bottom) [^{13}C]-A (1.0 mM), [^{13}C,^{15}N]-C (0.8 mM), [^{13}C]-G (1.0 mM), and [^{13}C,^{15}N]-U (0.7 mM). Assignments for carbon classes and selected individual signals are indicated.

A residues and several of the 10 G residues are apparent. It should be noted that several resonances are split by ^{13}C–^{13}C coupling constants of 60–75 Hz, including the C4 and C6 positions of A (Figure 2). The lowest spectral dispersion is exhibited by the resonances of C, which is largely a consequence of the RNA sequence. ΔTAR29.1 is purine-rich on one side of the duplex and pyrimidine-rich on the other (Figure 1), with all but two C residues in the A-form stem regions, so that the differences in base stacking which are the primary determinants of aromatic ^{13}C shifts (LaPlante et al., 1988) are minimal. Curiously, the A C6 and G C2 signals are very poorly resolved, despite the general dispersion of their other resonances. The most downfield C8 signal (142.7 ppm) derives from A35, as does the most downfield A C2 signal (155.5 ppm). The most downfield C C6, G C8, and U C6 signals belong to C24, G32, U25, and U31, respectively. All of these downfield resonances derive from nucleotides of the bulge or loop regions of the RNA, where stacking is expected to be weaker or nonexistent. With this clear correlation between aromatic ^{13}C shift and local environment, we hope that further integration of theoretical and experimental analysis will permit this information to be incorporated into RNA structure determination, where a more accurate description of partial stacking interactions would be helpful in understanding local conformational determinants.

The advantages of selective labeling become more apparent when two-dimensional ^1H–^{13}C spectra are considered, as shown for the ribose correlations in Figure 3. Although unresolved in these spectra, ^{13}C–^{13}C couplings of approximately 40 Hz are present in the ^{13}C (F_1) dimension but can be eliminated by application of constant-time methods if desired (Santoro & King, 1992). As observed for the aromatic signals, ribose correlations from the C residues of ΔTAR29.1 are less-resolved than others, making signal assignment by two- or three-

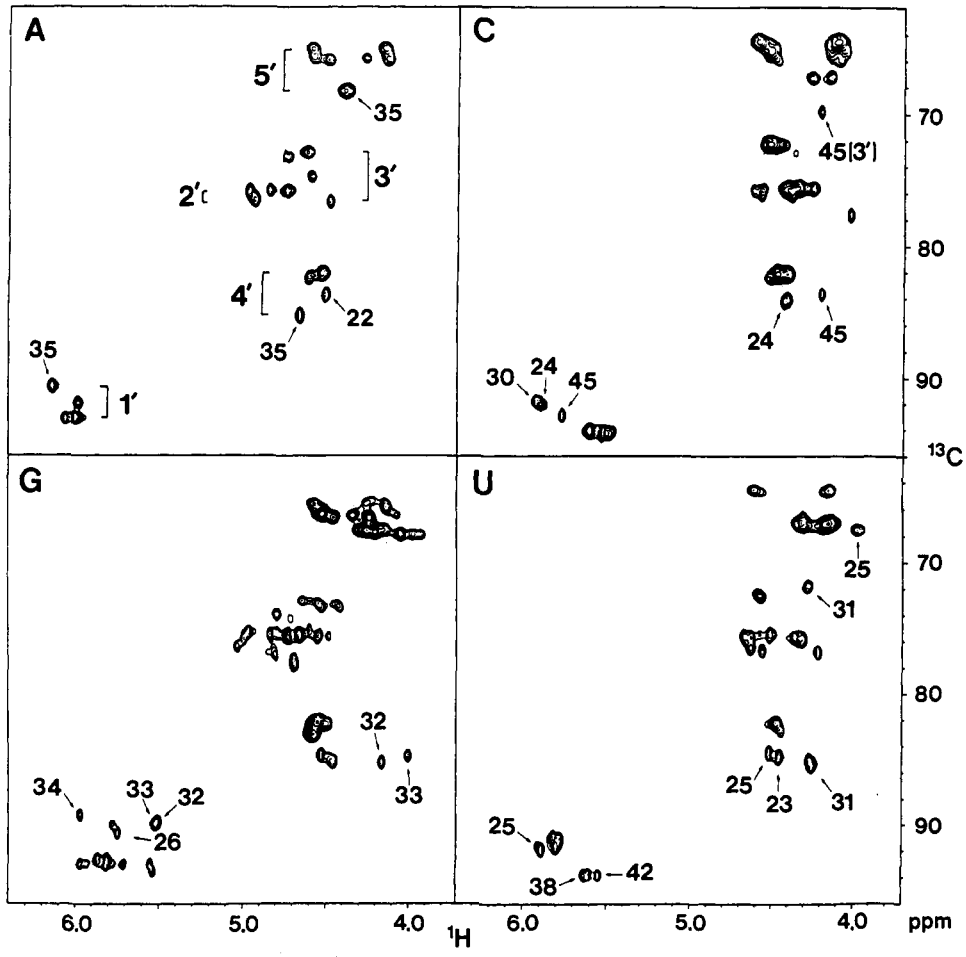

FIGURE 3: Ribose regions from ^{1}H–^{13}C HMQC and HSQC spectra of selectively labeled ΔTAR29.1. Chemical shift ranges and assignments to carbon classes are indicated for A residues. Some specific signal assignments are indicated in each panel. RNA samples are the same as those of Figure 2.

dimensional methods more difficult. Most notably, the chemical shifts of all four residue types display a tendency toward bifurcation in the ^{13}C dimension, as is most clearly evident for the C1′ signals of G and U. For A-labeled ΔTAR29.1, the ^{13}C chemical shifts of C1′, C2′, C3′, C4′, and C5′ range over 2.4, 1.0, 3.3, 3.2, and 2.7 ppm, respectively (Figure 3). When all residues are considered, it is apparent that ribose ^{13}C shifts for this molecule can range over 5 ppm for each carbon class. The observed bifurcation reflects populations representative of 3′-endo (N) or 2′-endo (S) conformations (Lankhorst et al., 1983), with a relatively few signals lying between the N and S limiting values (e.g., A22 C4′ and C45 C1′ in Figure 3). Movement of the average ribose conformation from the normal N state is associated with upfield shifts of C1′ signals and downfield shifts of all other ribose resonances. Because ^{13}C chemical shifts are much more easily and accurately measured than the ^{1}H–^{1}H coupling constants typically used to determine ribose conformations (Varani & Tinoco, 1991a), we propose that they be preferentially employed for larger RNAs. Using a small hairpin RNA, Varani and Tinoco (1991b) have demonstrated a general correlation between ^{1}H–^{1}H J coupling constants and ^{13}C chemical shifts obtained at natural abundance. Because several factors other than ribose pucker may also contribute to observed ^{13}C shifts, a measure which employs more than one chemical shift value is necessary to reduce or cancel these other effects. Combining our own limited data for ΔTAR29.1 with the results reported for a 12-mer hairpin (Varani et al., 1991; Varani & Tinoco, 1991b), we find an excellent linear correlation between ^{13}C shifts and the average ribose pseudorotation angle P for $0° < P < 180°$, the range of normal ribose ring puckers. The best correlation is displayed by ($\delta_{C1'} - \delta_{C4'}$), with a correlation coefficient of 0.94. We expect this relation to be refined in time, but it is already superior to the common use of a single homonuclear $^{3}J_{H1'H2'}$ value (Davis et al., 1990). Although NMR studies to date provide no good evidence for anything other than rapid N/S equilibria of RNA riboses in solution, it is possible that unusual ribose conformations may also be revealed by chemical shift analysis.

The spectral simplification afforded by selective labeling provides sufficient resolution for the application of 2D relaxation time experiments, which require signals to be monitored individually. Despite technical complications associated with ^{13}C–^{13}C coupling, preliminary relaxation experiments on ΔTAR29.1 have identified differences in atomic mobilities for residues of the stem, bulge, and loop regions (Xi and King, unpublished results). Better characterization of local atomic mobilities should both provide more accurate models of RNA solution structure and permit correlation of residue motions with recognition processes.

^{15}N NMR. Several previous NMR studies of labeled RNAs have exploited the $^{1}J_{^{15}N^{1}H}$ of approximately 90 Hz exhibited by the imino groups of G and U to examine hydrogen bonding within duplexes and tertiary interactions. Here we demonstrate that some important nonprotonated sites can also be monitored via the use of two-bond coupling. The N7 and N9 resonances of both purines and the N1 and N3 signals of A are easily identified through their medium-sized coupling (10–15 Hz) to H8 and H2, respectively. The N1 and N3 groups of A can provide a measure of internal hydrogen bonding and

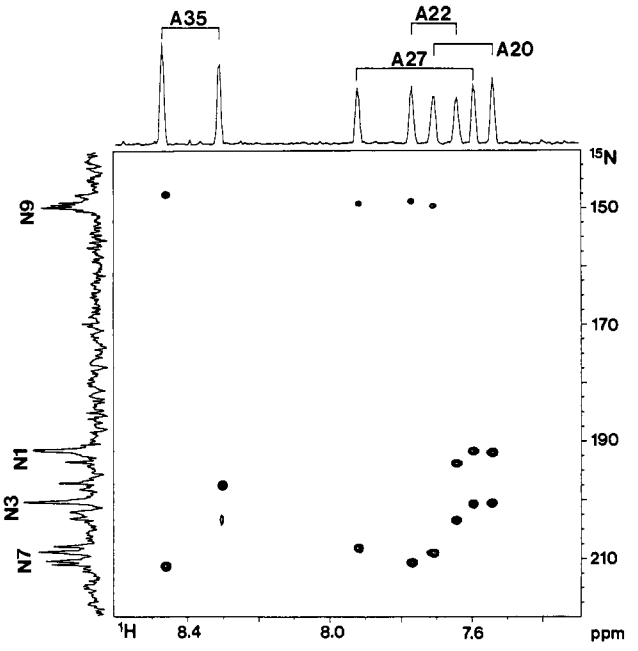

FIGURE 4: ^1H–^{15}N HMQC spectrum (τ = 10 ms) of 0.8 mM [^{15}N-A]ΔTAR29.1, with projection of the ^1H dimension and corresponding direct 1D spectrum for the ^{15}N dimension. Signal assignments for each residue and ^{15}N resonance class are indicated.

base stacking (James et al., 1981). The N1 groups of pyrimidines (and the purine N9s) can be also correlated with their H1′ protons. An example of the use of two-bond coupling to examine the four nonprotonated ring nitrogens of A is shown in Figure 4, where ^1H resonance assignments are derived from conventional sequential assignment procedures and ^{15}N assignments follow James et al. (1981). In all cases, the H2 signals for each A residue appear upfield of their corresponding H8 resonances.

For the TAR element, the ability to observe purine N7 sites is particularly important for the study of interactions at the major groove of the bulge, where the arginine-rich region of HIV-1 Tat protein, peptide fragments, and free arginine interact (Weeks & Crothers, 1991; Puglisi et al., 1992, and references cited therein). Recently, Delling et al. (1992) have proposed and Loret et al. (1992) have modeled a U23–G26–C39 base triple in free TAR. Puglisi et al. (1992) have used ^1H NMR to propose a transition between a partially stacked bulge and a U23–A27–U38 base triple upon argininamide binding. Since theoretical simulations indicate that discrimination between various bulge models using ^1H–^1H NOEs is difficult due to the relative paucity of interresidue NOEs at this site (Xi and King, unpublished results), we propose that heteronuclear chemical shift data will help to clarify NMR-derived structures at this and other sites. In free ΔTAR29.1, the ^{15}N (and ^{13}C) chemical shifts of A20 and A27 are very similar, consistent with their presence in duplex regions within a GAG sequence context. The similarity of the N7 shifts for A20 and A27 argues against the presence of a long-lived triple involving the latter residue in free TAR, since the formation of this structure would be expected to produce an upfield shift of significant magnitude (James et al., 1981). A similar argument also applies to G26, which displays a normal N7 chemical shift in the free species (data not shown). However, binding of the Tat-derived peptide YGRKKRRQRRRA results in a small shift of the A27 N7 signal, but a large (5 ppm) upfield shift of the G26 N7 signal, consistent with formation of a hydrogen bond between G26 and a charged arginine side chain in the Tat peptide, as suggested by Puglisi et al. (1992). Chemical shift changes due to hydrogen bonding are modified by stacking interactions, making it unclear whether ^{15}N chemical shift data can be reliably employed to detect the formation of isolated base triplets. However, the positive charge on the guanidinium group produces a stronger hydrogen bond and correspondingly larger shift than the uncharged and presumably weaker interaction in the U23–A27–U38 triple. The singularly large chemical shift change of the G26 N7 group upon Tat peptide binding is striking.

Heteronuclear chemical shift data also provide information on the structure of the TAR loop. The N7 (211.2 ppm), N3 (197.2 ppm), N1 (202.1 ppm), H2 (8.28 ppm), H8 (8.42 ppm), C2 (155.5 ppm), and C8 (142.7 ppm) signals of A35 (Figures 2 and 4) all appear substantially downfield of resonances from other A residues, consistent with substantial unstacking caused by extrusion of this base from the terminal loop structure. This suggestion is consistent with the results of 2D ^1H NMR studies (Chang, King, and Harper, unpublished results).

Conclusions. The labeling methods described here have generated immediately useful results for a biologically important RNA species. When applied in concert with existing pulse sequences and potential new experiments particular to the spin topology of nucleic acids, the greater spectral simplification provided by selective enrichment should make it a valuable addition to uniform labeling for the study of larger RNAs. With further development, coordinate analysis of ^1H, ^{13}C, ^{15}N, and ^{31}P chemical shift measurements in concert with ^1H–^1H NOEs will provide more reliable structural interpretation than can be obtained from ^1H signals alone, whether or not they are dispersed by a heteronuclear dimension. Analyses of several labeled RNAs presently being undertaken in various laboratories should provide sufficient data to test the validity of these proposals.

ACKNOWLEDGMENT

We thank Drs. Ding-Kwo Chang and Jorge Santoro for their assistance in the acquisition of NMR spectra and Naomi Logsdon for assistance with in vitro RNA synthesis.

REFERENCES

Batey, R. T., Inada, M., Kijawinski, E., Puglisi, J. D., & Williamson, J. R. (1992) *Nucleic Acids Res. 20*, 4515–4523.

Bax, A., Ikura, M., Kay, L. E., Torchia, D. A., & Tschudin, R. (1990) *J. Magn. Reson. 86*, 304–318.

Colvin, R. A., & Garcia-Blanco, M. A. (1992) *J. Virol. 66*, 930–935.

Davis, D. R., Yamaizumi, Z., Nishimura, S., & Poulter, C. D. (1989) *Biochemistry 28*, 4105–4108.

Davis, P. W., Adamiak, R. W., & Tinoco, I. (1990) *Biopolymers 29*, 109–122.

Delling, U., Reid, L. S., Barnett, R. W., Ma, M. Y.-X., Climie, S., Sumner-Smith, M., & Sonenberg, N. (1992) *J. Virol. 66*, 3018–3025.

Gewirth, D. T., Abo, S. R., Leontis, N. B., & Moore, P. B. (1987) *Biochemistry 26*, 5213–5220.

Gilman, M. (1987) in *Current Protocols in Molecular Biology*, pp 4.4.1–4.4.4, Wiley, New York.

Griffey, R. H., Davis, D., Yamaizumi, Z., Nishimura, S., Bax, A., Hawkins, B., & Poulter, C. D. (1985) *J. Biol. Chem. 260*, 9734–9741.

Harper, J. W., & Logsdon, N. (1991) *Biochemistry 30*, 8060–8066.

Hoard, D. E., & Ott, D. G. (1965) *J. Am. Chem. Soc. 87*, 1785–1788.

Ingraham, J. L., Maaløe, O., & Neidhardt, F. C. (1983) *Growth of the Bacterial Cell*, Sinauer Associates, Sunderland.

James, T. L., James, J. L., & Lapidot, A. (1981) *J. Am. Chem. Soc. 103*, 6748–6750.
Kime, M. J. (1984) *FEBS Lett. 173*, 342–346.
Lankhorst, P. P., Erkelenes, C., Haasnoot, C. A. G., & Altona, C. (1983) *Nucleic Acids Res. 11*, 7215–7230.
LaPlante, S. R., Boudreau, E. A., Zanatta, N., Levy, G. C., Borer, P. N., Ashcroft, J., & Cowburn, D. (1988) *Biochemistry 27*, 7902–7909.
Loret, E. P., Georgel, P., Johnson, W. C., & Ho, P. S. (1992) *Proc. Natl. Acad. Sci. U.S.A. 89*, 9734–9738.
Milligan, J. F., & Uhlenbeck, O. C. (1989) *Methods Enzymol. 180*, 51–62.
Milligan, J. F., Groebe, D. R., Witherall, G. W., & Uhlenbeck, O. C. (1987) *Nucleic Acids Res. 15*, 8783–8798.
Muesing, M. A., Smith, D. H., & Capon, D. J. (1987) *Cell 48*, 691–701.
Nikonowicz, E. P., & Pardi, A. (1992) *Nature 355*, 184–186.
Nikonowicz, E. P., Sirr, A., Legault, P., Jucker, F. M., Baer, L. M., & Pardi, A. (1992) *Nucleic Acids Res. 20*, 4507–4513.
Olsen, J. I., Schweizer, M. P., Walkiw, I. J., Hamill, W. D., Horton, W. J., & Grant, D. M. (1982) *Nucleic Acids Res. 10*, 4449–4464.
Polson, A. G., Crain, P. F., Pomerantz, S. C., McCloskey, J. A., & Bass, B. L. (1991) *Biochemistry 30*, 11507–11514.
Puglisi, J. D., Tan, R., Calnan, B. J., Frankel, A. D., & Williamson, J. R. (1992) *Science 257*, 76–80.
Roy, S., Papastavros, M. Z., Sanchez, V., & Redfield, A. G. (1984) *Biochemistry 23*, 4395–4400.
Rosen, C. A., Sodroski, J. G., & Haseltine, W. A. (1985) *Cell 41*, 813–823.
Santoro, J., & King, G. C. (1992) *J. Magn. Reson. 97*, 202–207.
Schmidt, P. G., Sierzputowska-Gracz, H., & Agris, P. F. (1987) *Biochemistry 26*, 8529–8534.
Simon, E. S., Grabowski, S., & Whitesides, G. M. (1990) *J. Org. Chem. 55*, 1834–1841.
Summers, W. C. (1970) *Anal. Biochem. 33*, 459–463.
Szewczak, A. A., White, S. A., Gewirth, D. T., & Moore, P. B. (1990) *Nucleic Acids Res. 18*, 4139–4142.
Varani, G., & Tinoco, I. (1991a) *Q. Rev. Biophys. 24*, 479–532.
Varani, G., & Tinoco, I. (1991b) *J. Am. Chem. Soc. 113*, 9349–9354.
Varani, G., Cheong, C., & Tinoco, I. (1991) *Biochemistry 30*, 3280–3289.
Weeks, K. M., & Crothers, D. M. (1991) *Cell 66*, 577–588.
Wyatt, J. R., Puglisi, J. D., & Tinoco, I. (1989) *Bioassays 11*, 100–106.
Yokoyama, S., Usuki, K. M. J., Yamaizumi, Z., Nishimura, S., & Miyazawa, T. (1980) *FEBS Lett. 119*, 77–80.